Mixed-error approach for multi-channel active noise control of open windows

Tatsuya Murao[1], Chuang Shi[2*], Woon-Seng Gan[1], and Masaharu Nishimura[3]
[1] School of Electrical and Electronic Engineering, Nanyang Technological University, Singapore
[2] School of Electronic Engineering, University of Electronic Science and Technology of China, China
[3] Graduate School of Engineering, Tottori University, Japan
[*] Corresponding author's email: shichuang@uestc.edu.cn

Abstract: This paper presents an attempt to reduce the computational complexity, while achieving acceptable level of noise reduction in a multi-channel active noise control (MCANC) system for mitigating noise passing through open windows. The reference signals are sensed at the back of the secondary loudspeakers. The existing approach to reduce the computational complexity has already used only one reference signal in each feedforward channel. As the number of error microphones is also important to ensure global noise reduction of the MCANC system for open windows, the main idea of this paper is to preprocess the error signals so that the number of inputs to the controller is further reduced. When the preprocessing is a simple summation, it is called the mixed-error approach. The number of inputs related to the error signals is eventually reduced to 1 after the mixed-error approach is applied. Simulation results demonstrate that the optimum control filters derived under general conditions can lead to similar global noise reduction to those derived based on the mixed-error approach. Experimental results confirm that in a 4-channel MCANC system applied to a 0.2 m by 0.2 m open window, the performance of global noise reduction is not compromised by the mixed-error approach.

Keywords: *multi-channel active noise control, feedforward FxLMS algorithm, mixed-error approach, open window*

1. INTRODUCTION

Active noise control (ANC) techniques have been widely used in many noise mitigating applications [1, 2], such as reducing tonal noise in an aircraft cabin [3], cancelling airflow noise in a duct [4], treating engine noise in vehicles [5]. ANC techniques are favorable when dealing with low-frequency noise, whereby passive noise control techniques may fail to provide efficient noise reduction [6]. Most of the ANC applications focus on the local cancellation of noise in a small region, exemplified by noise cancelling headphones. Within one tenth of the noise wavelength from the error microphone location, a reduction of 10 dB in the noise level is typically obtained [7]. However, there is a recent trend of extending the control region to achieve global noise reduction by multi-channel active noise control (MCANC) systems [8-13].

In previous studies, we have proposed the concept to achieve global noise reduction in a room by deploying an MCANC system at the opening window [14-17]. Each feedforward channel of this MCANC system consists of a reference microphone and a secondary loudspeaker, as depicted in Fig. 1. The reference microphones face outwards, while the secondary loudspeakers face inwards. The feedforward channels are configured uniformly in the middle of the open window. According to Ise's boundary surface control principle, the sound field in an enclosed space can be controlled by adjusting the sound pressure and particle velocity on the surface of the space [18, 19]. Therefore, the MCANC system for open windows is feasible to generate the anti-noise field with inverted phase of the noise field, so that the noise level in the room is globally minimized.

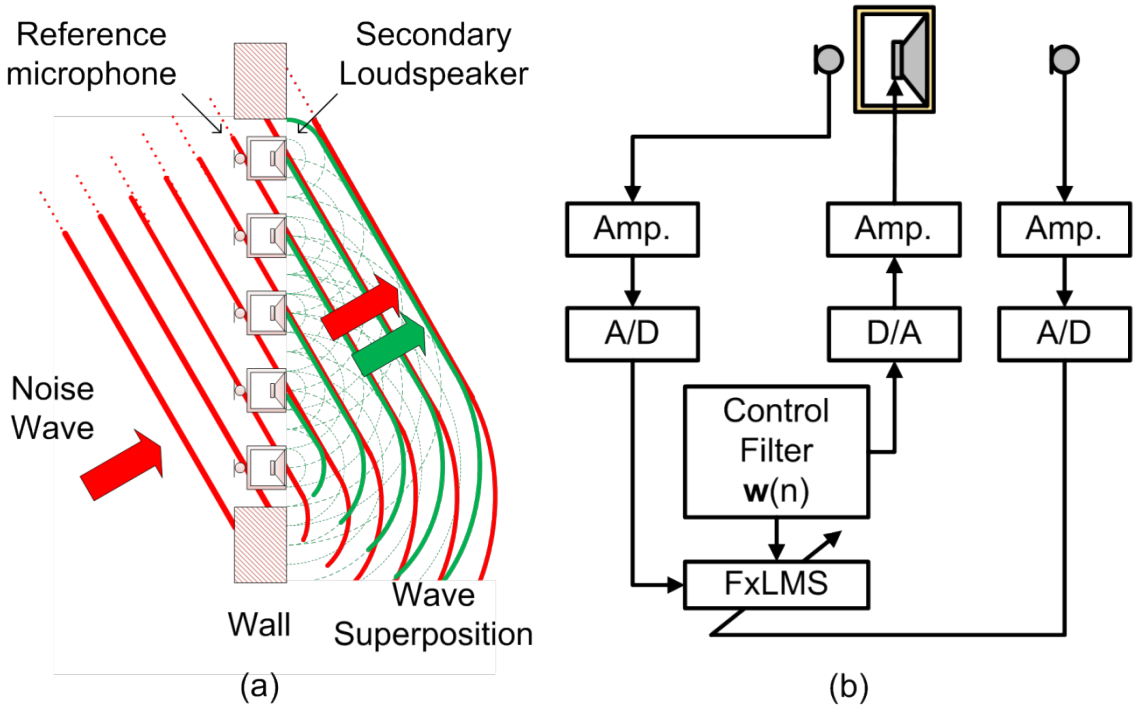

Fig. 1 MCANC system to mitigate noise passing through an open window: (a) illustration of wave superposition; (b) block diagram of a single-channel feedforward ANC system.

There are several design parameters of the MCANC system for open windows. Firstly, the size of the secondary loudspeaker may block natural ventilation. It also affects the lower effective frequency bound of the system, as small-sized loudspeakers usually cannot generate low-frequency sound at sufficiently high levels [17]. Secondly, the separation between the secondary loudspeakers determines the spatial aliasing condition, which provides the upper effective frequency bound of the system. Thirdly, the distance from the reference microphone to the secondary loudspeaker limits the maximum processing time as a result of the causality constraint of feedforward ANC systems, whereby the driving signal of the secondary loudspeaker has to be generated before the actual noise wave reaches the position of the secondary loudspeaker. On the other hand, a shorter distance from the reference microphone to the secondary loudspeaker is more favorable to carry out the decentralized MCANC algorithms that are much less complicated than the centralized MCANC algorithm [15-17]. In those decentralized MCANC algorithms, the control signal

of each secondary loudspeaker is generated based on only one reference signal that is sensed by the nearest reference microphone. This is also known as the collocated implementation. When the distance from the reference microphone to the secondary loudspeaker is relatively longer, the decentralized MCANC algorithms are less effective for the moving noise source and multiple noise sources [14]. A compromise between the processing time and performance of the decentralized MCANC algorithms is to adopt a high sampling frequency. However, the high sampling frequency results in high computational complexity, due to the fact that the filter tap length is increased to maintain the frequency resolution.

In this paper, we propose to use the mixed-error approach to reduce the computational complexity, while achieving acceptable level of noise reduction in the MCANC system for open windows. The mixed-error approach simplifies the MCANC system to parallel single-channel feedforward ANC systems, whereby each single-channel feedforward ANC system takes the summed output of an error microphone array as the error signal [20]. The mixed-error approach has the merit of very low computational complexity as compared to the complete implementation of the MCANC system. When the summation of the error microphones' outputs is carried out by an analog mixer, the number of analog-to-digital convertors (ADCs) is also greatly reduced. There are previous works carrying out the mixed-error approach in feedback ANC systems [21-23]. It is of interest to compare the mixed-error approach with the mixed-reference approach, as in feedback ANC systems both approaches are coupled. However, in the MCANC system for open windows, the collocated implementation already uses only one reference signal in each channel. The mixed-reference approach cannot further reduce the computational complexity in the collocated implementation of the MCANC system. Furthermore, a weighted summation appears to be a more generic theoretical framework for such mixed-error and mixed-reference approaches [23], since the sensitivity of every microphone may not be exactly the same in practice.

2. MCANC ALGORITHMS

The MCANC system, shown in Fig. 2, includes I reference microphones, J secondary loudspeakers, and K error microphones, which is also called the $I \times J \times K$ MCANC system. The reference signal vector of the i-th reference microphone is denoted as

$$\mathbf{x}_i(n) = \left[x_i(n), x_i(n-1), \cdots, x_i(n-L+1)\right]^T, \tag{1}$$

where L is the tap length for both the control filters and secondary path models. The control filter that calculates the output of the j-th secondary loudspeaker based on the input from the i-th reference microphone is denoted as

$$\mathbf{w}_{ji}(n) = \left[w_{ji}^{(0)}(n), w_{ji}^{(1)}(n), \cdots, w_{ji}^{(L-1)}(n)\right]^T. \tag{2}$$

The output of the j-th secondary loudspeaker is denoted as

$$\mathbf{y}_j(n) = \left[y_j(n), y_j(n-1), \cdots, y_j(n-L+1)\right]^T, \tag{3}$$

where

$$y_j(n) = \sum_{i=1}^{I} \mathbf{w}_{ji}^T(n)\mathbf{x}_i(n). \tag{4}$$

Therefore, the error signal measured at the k-th error microphone is a summation of the noise and anti-noise signals as

$$e_k(n) = d_k(n) + \sum_{j=1}^{J} \mathbf{s}_{kj}^T \mathbf{y}_j(n), \tag{5}$$

where $d_k(n)$ is the noise signal received by the k-th error microphone. Moreover, the secondary path from the j-th secondary loudspeaker to the k-th error microphone is denoted as

$$\mathbf{s}_{kj} = \left[s_{kj}^{(0)}, s_{kj}^{(1)}, \cdots, s_{kj}^{(L-1)}\right]^T. \tag{6}$$

In order to update the control filters, the multi-channel FxLMS algorithm is adopted as

$$\mathbf{w}_{ji}(n+1) = \mathbf{w}_{ji}(n) - \mu \sum_{k=1}^{K} [e_k(n)\mathbf{r}_{kji}(n)], \tag{7}$$

where the filtered reference signal vector is written as

$$\mathbf{r}_{kji}(n) = \left[r_{kji}(n), r_{kji}(n-1), \cdots, r_{kji}(n-L+1) \right]^T. \tag{8}$$

Each element in (8) is calculated by

$$r_{kji}(n) = \hat{\mathbf{s}}_{kj}^T \mathbf{x}_i(n). \tag{9}$$

Here, an estimate of the secondary path, assumed to be obtained offline, is written as

$$\hat{\mathbf{s}}_{kj} = \left[\hat{s}_{kj}^{(0)}, \hat{s}_{kj}^{(1)}, \cdots, \hat{s}_{kj}^{(L-1)} \right]^T. \tag{10}$$

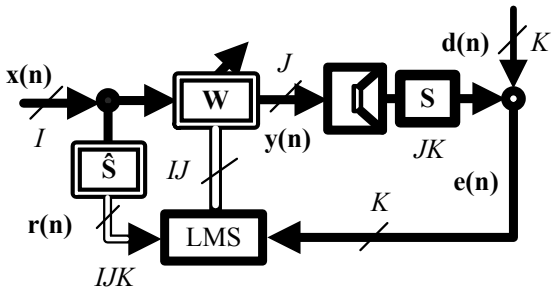

(a) Complete implementation of FxLMS algorithm

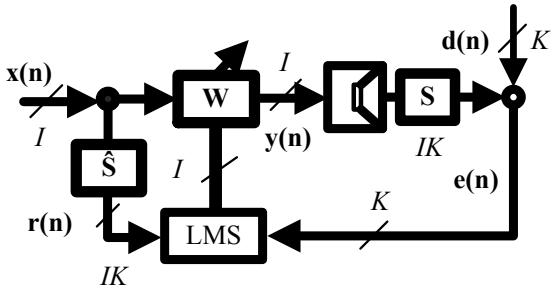

(b) Collocated implementation of FxLMS algorithm

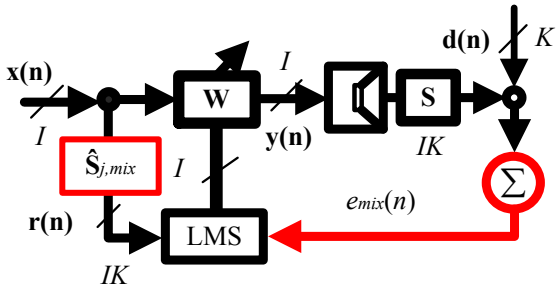

(c) Mixed-error implementation of FxLMS algorithm

Fig. 2 Block diagram of different implementations of the MCANC system.

The complete implementation of the MCANC system, illustrated in Fig. 2(a), is heavily computationally complicated. There are $I \times J$ control filters in total and each control filter is updated by K error signals. It is noteworthy that the feedback path cancellation is not included in the block diagram. The feedback path cancellation helps to improve the stability of the MCANC system. However, the computational complexity of the multi-channel feedback path cancellation can be overwhelming. Whether to implement the feedback path cancellation is often decided by the characteristics of the feedback paths. In previous studies [14-16], though being drawn in the block diagram, the feedback path cancellation is not actually implemented. Therefore, this paper follows the practice to remove the feedback path cancellation in the MCANC system for open windows.

The MCANC system for open windows usually uses the same number of reference microphones and secondary loudspeakers, i.e. $I = J$ as shown in Fig. 2(b). As aforementioned, the existing approach to reduce the computational complexity is to adopt a simplification that the output of each secondary loudspeaker is calculated merely based on the input from the nearest reference microphone, i.e.

$$y_i(n) = \mathbf{w}_{ii}^T(n)\mathbf{x}_i(n). \tag{11}$$

Each pair of such secondary loudspeaker and reference microphone forms a collocated feedforward channel. The trade-off of using the collocated channels is the reduced number of effective reference signals, which in turn reduces the noise reduction performance when there are many noise sources or the noise source is moving [17]. The coefficient updating equation of the i-th channel is given by

$$\mathbf{w}_{ii}(n+1) = \mathbf{w}_{ii}(n) - \mu \sum_{k=1}^{K} [e_k(n)\mathbf{r}_{kii}(n)]. \tag{12}$$

When the collocated implementation of the MCANC system is practically allowed, the computational complexity is $1/M$ as much as that of the complete implementation. There are only I control filters, but each of the control filter is still updated with K error signals.

To further reduce the computational complexity, the number of error microphones can be saved by combining them into groups so that the controller only receives one input from each group. In this paper, we refer to the summation of the outputs of all the error microphones as the mixed-error signal, which is written as

$$e_{mix}(n) = \sum_{k=1}^{K} e_k(n) = \sum_{k=1}^{K} \left(d_k(n) + \sum_{j=1}^{J} \mathbf{s}_{kj}{}^{T} \mathbf{y}_j(n) \right). \tag{13}$$

When the mixed-error signal is used to update the control filters, the computational complexity is reduced by K times. The actual number of error microphones is unchanged to keep the MCANC system reliable, as shown in Fig. 2(c). When the summation is carried out by an analog mixer, the number of ADCs is also reduced by K times, as only one ADC is needed for sampling the mixed-error signal.

The coefficient updating equation of the i-th channel is now given by

$$\mathbf{w}_{ii}(n+1) = \mathbf{w}_{ii}(n) - \mu e_{mix}(n) \mathbf{r}_{mix,i}(n), \tag{14}$$

where

$$\mathbf{r}_{mix,i}(n) = \left[r_{mix,i}(n), r_{mix,i}(n-1), \cdots, r_{mix,i}(n-L+1) \right]^T \tag{15}$$

and

$$r_{mix,i}(n) = \hat{\mathbf{s}}_{mix,i}^T \mathbf{x}_i(n). \tag{16}$$

It is noteworthy that the mixed secondary path estimate $\hat{\mathbf{s}}_{mix,i}$ is measured from the i-th secondary loudspeaker with respect to the mixed-error signal. Furthermore, the mixed-error approach is not limited to the collocated implementation of the MCANC system. It is also feasible to the complete implementation.

The optimum FxLMS control filters using the mixed-error approach satisfy

$$\frac{\partial e_{mix}^2(n)}{\partial \mathbf{w}_{ij}} = 2 e_{mix}(n) \frac{\partial e_{mix}(n)}{\partial \mathbf{w}_{ij}} = 2 \left[\sum_{k=1}^{K} e_k(n) \right] \left[\sum_{k=1}^{K} \frac{\partial e_k(n)}{\partial \mathbf{w}_{ij}} \right] = 0, \tag{17}$$

whilst the normal optimum FxLMS control filters lead to

$$\frac{\partial \sum_{k=1}^{K} e_k^2(n)}{\partial \mathbf{w}_{ij}} = 2\sum_{k=1}^{K}\left[e_k(n)\frac{\partial e_k(n)}{\partial \mathbf{w}_{ij}} \right] = 0. \tag{18}$$

Comparing (17) and (18), we could find mathematically that only when

$$\left[\sum_{k=1}^{K} e_k(n)\right]\left[\sum_{k=1}^{K}\frac{\partial e_k(n)}{\partial \mathbf{w}_{ij}}\right] \propto \sum_{k=1}^{K}\left[e_k(n)\frac{\partial e_k(n)}{\partial \mathbf{w}_{ij}} \right] \tag{19}$$

i.e.

$$\sum_{m=1}^{K}\sum_{n=1}^{K}\left[e_m(n)\frac{\partial e_n(n)}{\partial \mathbf{w}_{ij}} \right] \propto \sum_{k=1}^{K}\left[e_k(n)\frac{\partial e_k(n)}{\partial \mathbf{w}_{ij}} \right] \quad \text{for } m \neq n, \tag{20}$$

the mixed-error approach can converge to the same optimum control filters as those of the normal FxLMS algorithm. This could happen when the output of every error microphone is almost identical, for example when the incidence angle of the noise wave is 0 degree [16].

Table I present the computational complexity of the complete, collocated, and mixed-error implementations of the MCANC system. When $I = J = K$ and $L = 100$ taps, Fig. 3 shows the number of multipliers used in different implementations with respect to the number of channels. If the computational power of a controller is able to handle the complete implementation of the 4-channel FxLMS algorithm with above settings, it is also feasible to run the collocated implementation of the 8-channel FxLMS algorithm or even up to the 48-channel FxLMS algorithm with the mixed-error approach.

Table I. Computational complexity of complete, collocated, mixed-error implementations of the multi-channel FxLMS algorithm with no feedback path cancellation.

	Generating secondary signals	Calculating filtered-x signals	Updating control filters	Total computational cost
Complete $I \times J \times K$	IJL_w	$IJKL_s$	$IJK\left(L_w+1\right)$	$IJ\left[K\left(L_s+1\right)+\left(K+1\right)L_w\right]$
Collocated $I(1\times1)\times K$	IL_w	IKL_s	$IK\left(L_w+1\right)$	$I\left[K\left(L_s+1\right)+\left(K+1\right)L_w\right]$
Mix-error $I(1\times1)\times1_{mix}$	IL_w	IL_s	$I\left(L_w+1\right)$	$I\left[\left(L_s+1\right)+2L_w\right]$

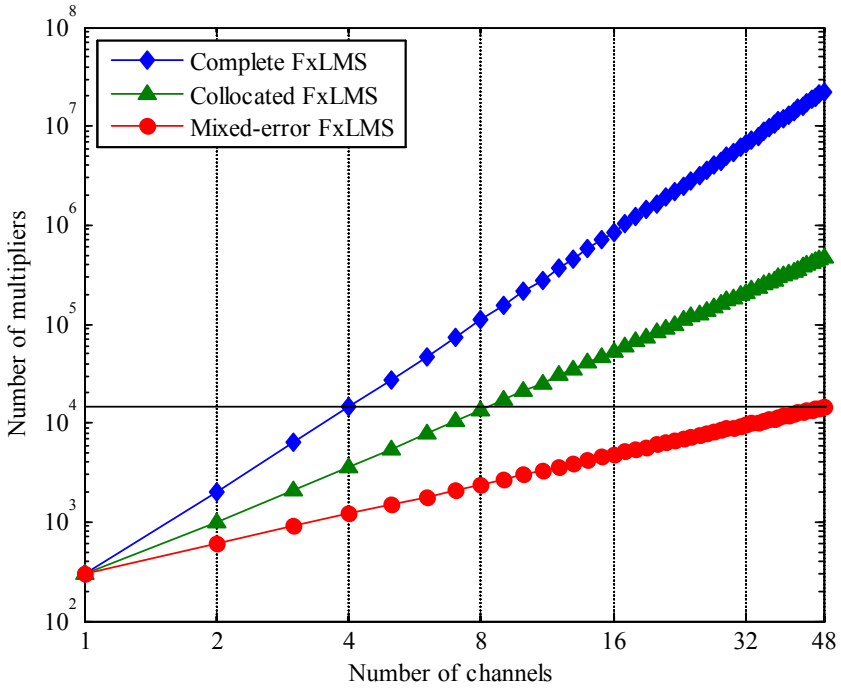

Fig. 3 Total number of multipliers in complete, collocated, mixed-error implementations of the multi-channel FxLMS algorithm with no feedback path cancellation, where $I = J = K$ and $L = 100$ taps are adopted.

3. SIMULATION RESULTS

To validate the noise reduction performance of different implementations of the MCANC system for open windows, a simplified time domain simulation is configured in three-dimensional free field. All the secondary loudspeakers and microphones are assumed

as point sources and omnidirectional sensors. The transfer function between any two points is merely a function of the distance. Perfect secondary path estimates are also assumed, i.e. $\hat{\mathbf{s}}_{kj} = \mathbf{s}_{kj}$. The primary noise is set as a plane wave, starting from the plane where the reference microphones are distributed. Thus, perfect reference signals and feedback cancellations are also implicitly assumed. The tap length of the control filters are set sufficiently long to ensure optimum performance, as the computational time is not a concern of the simulation.

The sampling frequency and the speed of sound in air are set as 48 kHz and 340.5 m/s, respectively. The frequency band of the primary noise is limited from 0.5 to 2 kHz. The reference microphones, secondary loudspeakers, and error microphones are configured as 2 by 2 square arrays. The spacing between the reference microphones, secondary loudspeakers, and error microphones are all set to u = 0.1206 m, which equals to the distance that a sound wave travels during the time duration of 17 samples. The distance from the center of the reference microphones to the center of the secondary loudspeakers is set as a = 0.05675m, which equals to the distance that a sound wave travels during the time duration of 8 samples. The distance from the center of the secondary loudspeakers to the center of the error microphones is set at b = 1u, 2u, 5u, and 10u to examine the effect of the error microphone position on the noise reduction performance. The incidence angle of the primary noise is preliminarily fixed at 0 degree. This setting is chosen based on the experimental observations in [14], suggesting that the control filters trained with the normal incidence angle remain effectively for other incidence angles. The simulation results are collected in a horizontal square of 5 m by 5 m. The geometry of the simulation setup is drawn in Fig. 4.

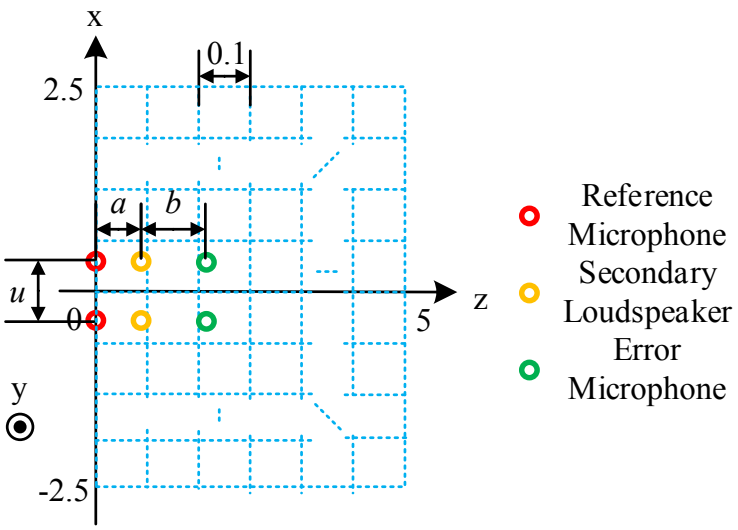

Fig. 4 Geometry of the simulation setup.

The power spectra at the error microphone are shown in Fig. 5. As the incidence angle of the primary noise is 0 degree, the output of every error microphone is very similar. In this case, the mixed-error implementation of the FxLMS algorithm can lead to almost identical control filters as those of the collocated implementation. The slight difference in the error spectra between the mixed-error and collocated implementations is likely to be caused by the uncertain residual error of the adaptation process.

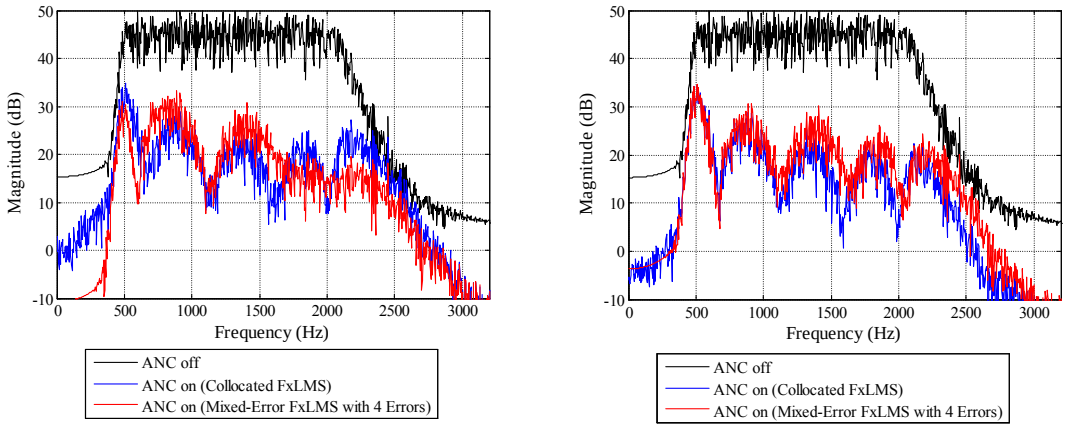

(a) Error microphone position of 1*u*

(b) Error microphone position of 2*u*

(c) Error microphone position of 5*u*

(d) Error microphone position of 10*u*

Fig. 5 Power spectra at different error microphone positions.

The contour plots of the noise reduction are shown in Fig. 6. The noise reduction is calculated as the averaged reduction across all the frequency bins within the frequency range of the primary noise. Global noise reduction performance is mainly determined by the position of the error microphone, rather than the algorithm's implementation. This indicates that the mixed-error approach can be useful in practice when the global noise reduction is the objective and the computational complexity is the major concern.

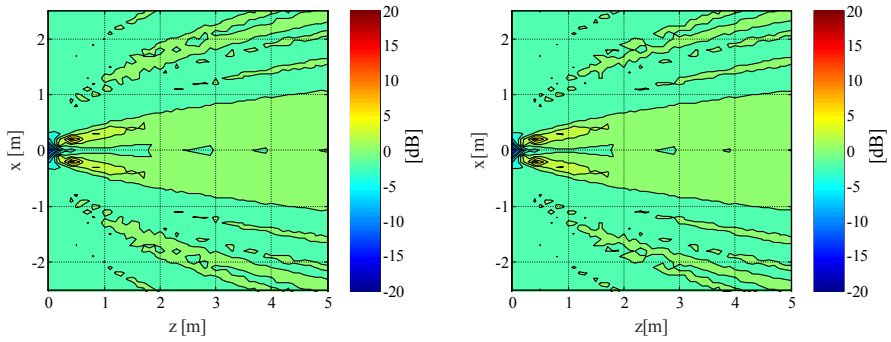

(a) Collocated FxLMS (1*u*)

(b) Mixed-Error FxLMS (1*u*)

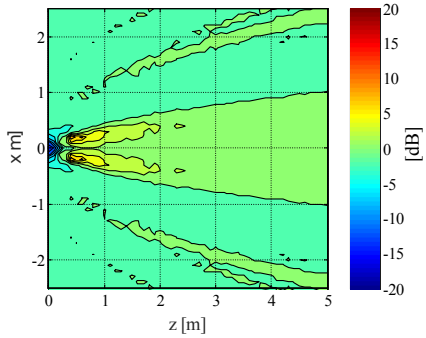

(c) Collocated FxLMS (2*u*)

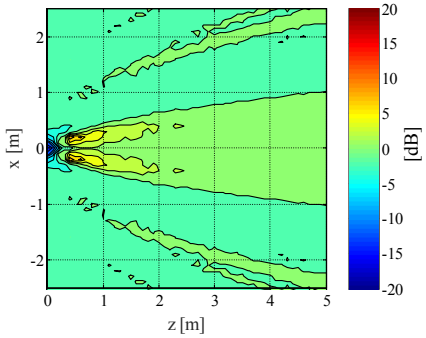

(d) Mixed-Error FxLMS (2*u*)

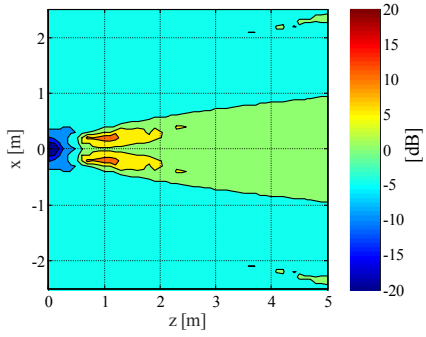

(e) Collocated FxLMS (5*u*)

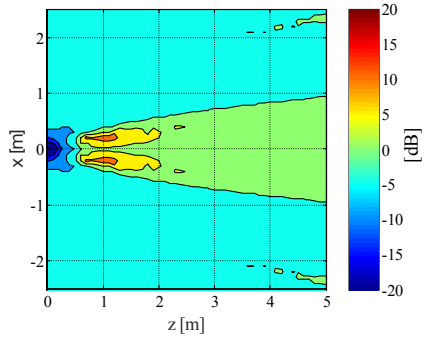

(f) Mixed-Error FxLMS (5*u*)

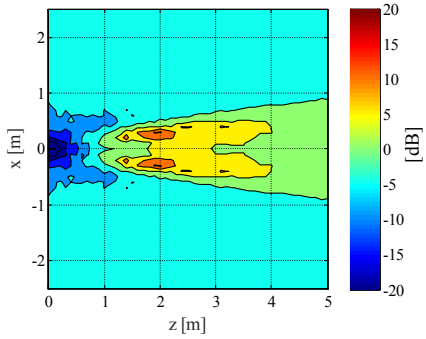

(g) Collocated FxLMS (10*u*)

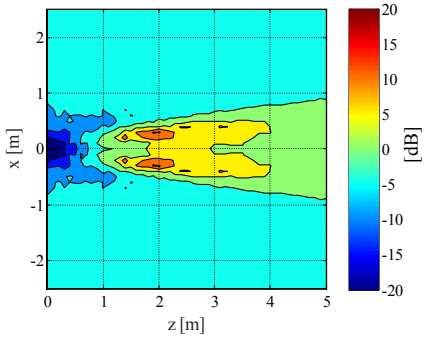

(h) Mixed-Error FxLMS (10*u*)

Fig. 6 Noise reduction contour plots of the collocated and mixed-error implementations of the 4-channel FxLMS algorithm.

4. EXPERIMENTAL RESULTS

The experimental setup is illustrated in Fig. 7. The primary noise, transmitted by an enclosed loudspeaker, is a band-limited random noise from 0.4 to 1.6 kHz. This frequency band is decided by the measured characteristics of the miniature loudspeakers used in the experiment. The opening on the enclosure allows the primary noise to pass through and 4 secondary loudspeakers are distributed on the opening. The size of the opening is 0.2 m by 0.2 m. The spacing between the secondary loudspeakers is 0.1 m. Therefore, the upper frequency bound is given by the Nyquist frequency at about 1.7 kHz. The reference microphones are located inside the enclosure, with a distance of 0.12 m from the closest secondary loudspeaker. The error microphones are placed outside the enclosure. The distance from the center of the error microphones to the center of the open window is manually moved from 0.1 m to 1 m. The numbers of error microphones are selected as 4 (No. 1 to No. 4) and 8 (No. 1 to No. 8). The noise reduction performance is measured under different arrangements.

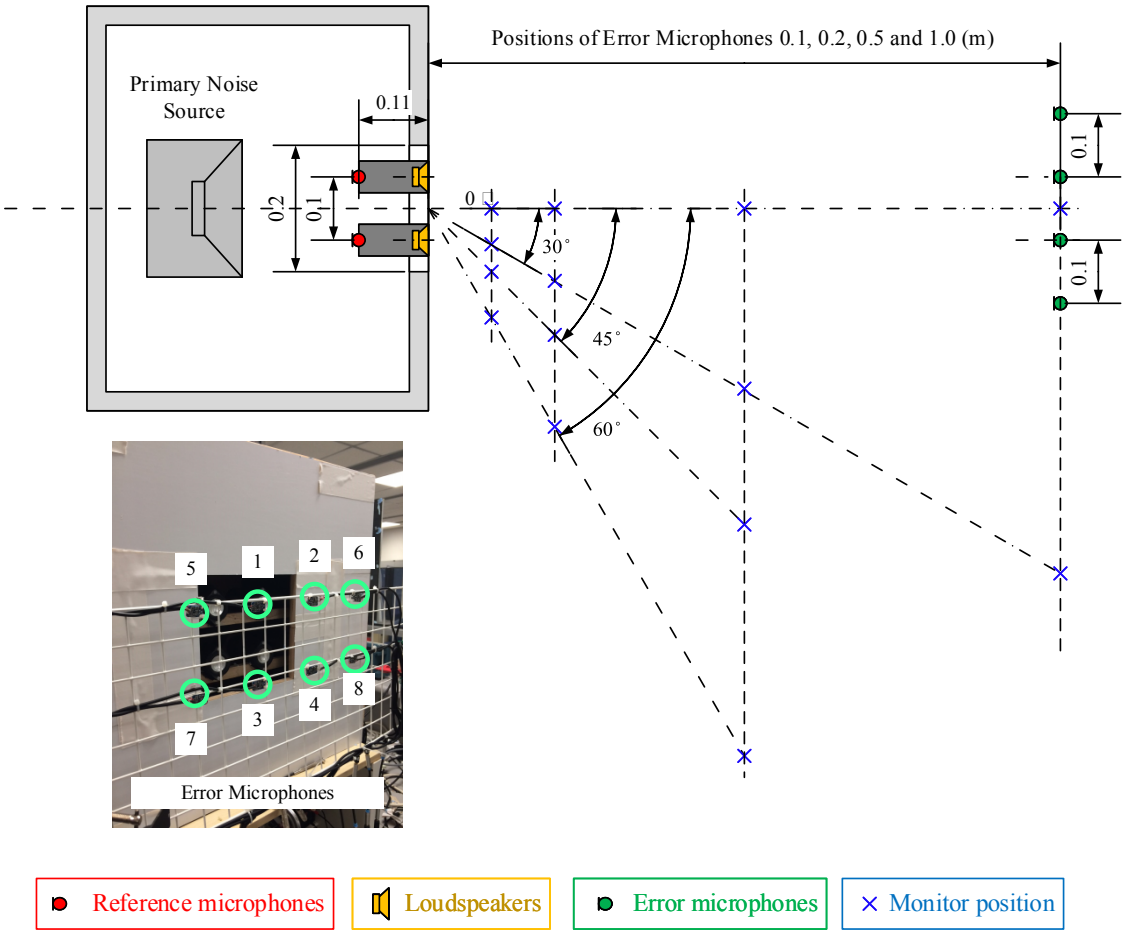

Fig. 7 Experimental setup.

The controller is a Texas Instrument TMS320C6713 DSP Starter Kit running at 225 MHz clock rate. The 16 bit ADCs and DACs are integrated on the HEG DSK6713 IF-A data acquisition board, supporting up to 200 kHz sampling frequency. The actual sampling frequency is set to 16 kHz and the cut-off frequency of anti-aliasing and reconstruction filters is made to 8 kHz. The selection of a relatively high sampling frequency caters for the short distance between the reference microphone and secondary loudspeaker in every channel. Increasing the sampling frequency reduces the hardware latency and therefore allows a reduced distance between the reference microphone and secondary loudspeaker in the feedforward ANC system. The tap lengths of the control filters and secondary path estimates are 100 taps for the collocated implementation, while the tap lengths of the control

filterers are increased to 200 taps for the mixed-error implementation to fully utilize the computational power of the controller. An analog mixer is used to sum the error signals to reduce the number of ADCs. Both secondary paths and the mixed-error secondary path are identified offline with a white noise excitation.

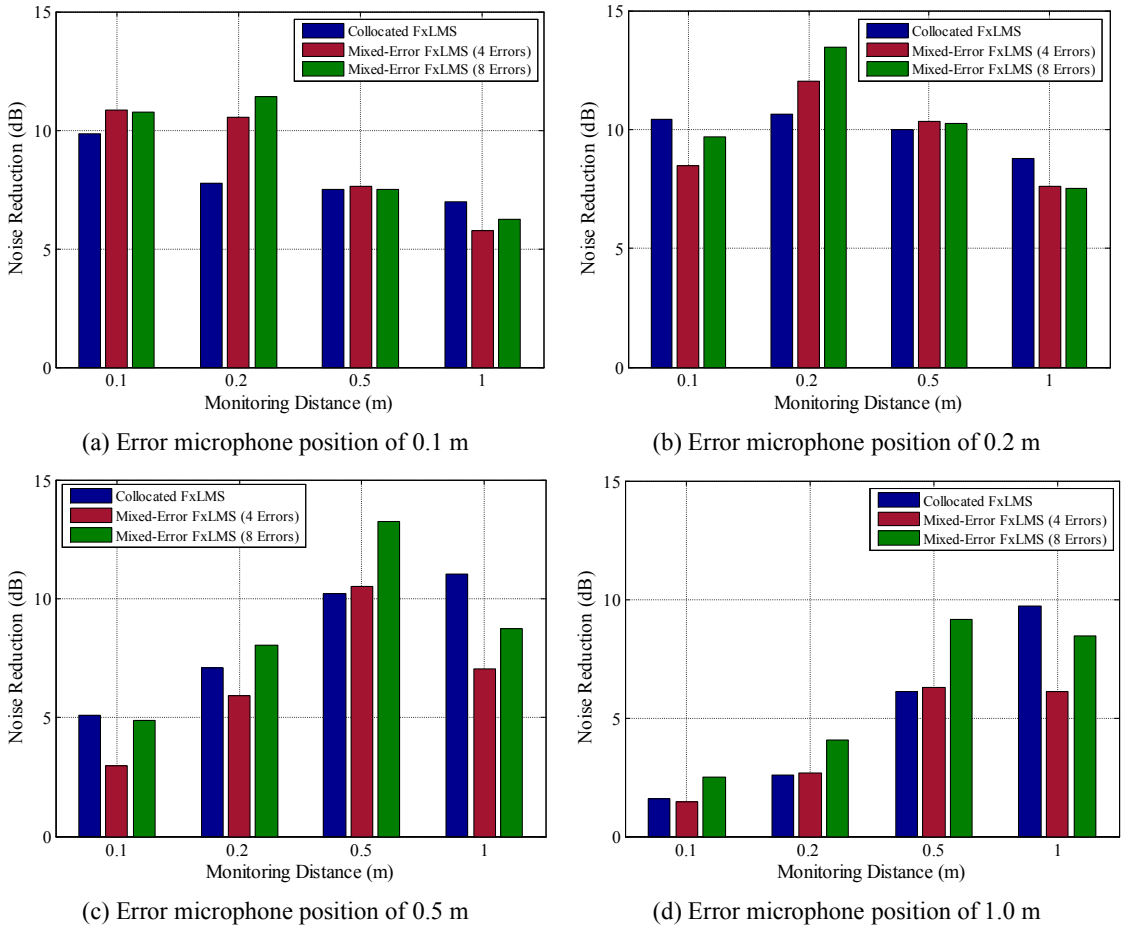

(a) Error microphone position of 0.1 m

(b) Error microphone position of 0.2 m

(c) Error microphone position of 0.5 m

(d) Error microphone position of 1.0 m

Fig. 8 Noise reduction performance at the observation points when the error microphones are placed on the 0-degree axis at a distance of (a) 0.1 m; (b) 0.2 m; (c) 0.5 m; (d) 1.0 m from the open window.

Figure 8 shows the noise reduction performance when the error microphones are placed at different distances on the 0-degree axis. The collocated implementation can only be carried out with 4 error microphones, but the mixed-error implementation is attempted with 4 and 8 error microphones. Both the collocated and mixed-error implementations are measured after the sufficient convergence of the control filters. It is observed in Fig. 8 that

using more error microphones with the mixed-error approach improves the noise reduction performance on the 0-degree axis. When 8 error microphones are placed at a distance of 0.2 m from the open window, the mixed-error implementation achieves the best overall performance.

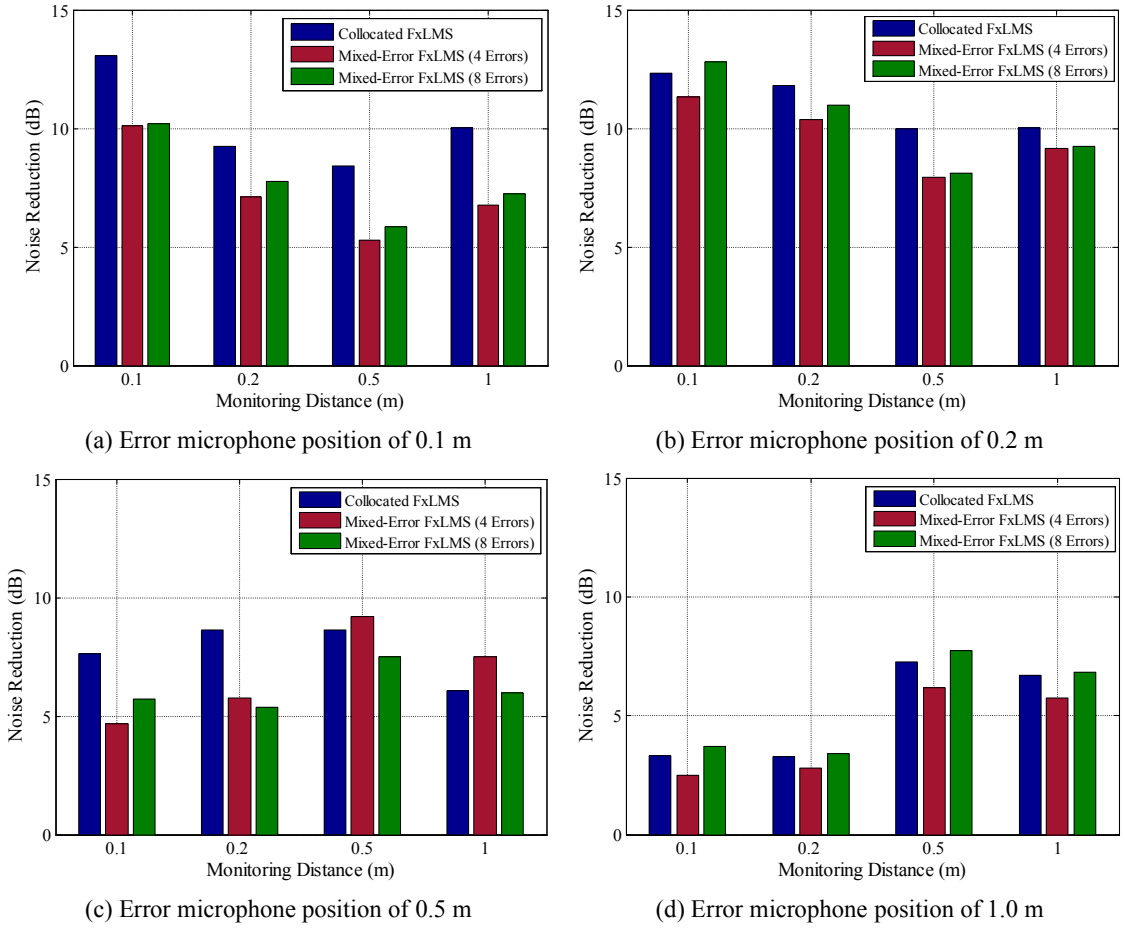

(a) Error microphone position of 0.1 m

(b) Error microphone position of 0.2 m

(c) Error microphone position of 0.5 m

(d) Error microphone position of 1.0 m

Fig. 9 Noise reduction performance at the observation points when the error microphones are placed on the 30-degree axis at a distance of (a) 0.1 m; (b) 0.2 m; (c) 0.5 m; (d) 1.0 m from the open window.

Figure 9 shows the noise reduction performance when the error microphones are placed at different distances on the 30-degree axis. The collocated implementation achieves slightly better noise reduction performance than the mixed-error implementation. However, placing the error microphones at a distance of 0.2 m from the open window can still provide

the best overall performance. More results measured on the 45-degree and 60-degree axes are listed in Table II. The mixed-error implementation with 8 error microphones placed at a distance of 0.2 m from the open window is demonstrated to be the most efficient combination.

Table II Noise reduction performance at the observation points when the error microphones were placed on the 45- and 60-degree axes at a distance of (a) 0.1 m; (b) 0.2 m; (c) 0.5 m; (d) 1.0 m from the open window

Implementation	Error microphone position from the open window (m)	Axial angle (degree) and Monitoring distance (m)					
		45 (degree)			60 (degree)		
		0.1 (m)	0.2 (m)	0.5 (m)	0.1 (m)	0.2 (m)	0.5 (m)
Collocated FxLMS	0.1	11.86	3.52	9.07	7.2	6.55	5.27
	0.2	10.16	8.68	7.66	5.57	6.4	3.11
	0.5	7.64	8.05	2.86	2	5.18	-0.43
	1	3.82	3.09	6.13	0.86	4.47	0.22
Mixed-error FxLMS (4 Errors)	0.1	8.31	4.98	6.31	7.66	5.24	3.11
	0.2	12.1	8.42	8.44	9.3	7.37	4.84
	0.5	5.06	6.29	6.42	3.09	8.45	2.5
	1	2.68	3.26	4.13	1.04	6.19	0.46
Mixed-error FxLMS (8 Errors)	0.1	8.02	5.46	6.07	5.72	5.63	2.06
	0.2	12.81	8.46	8.65	8.54	7.42	4.25
	0.5	5.9	5.61	5.4	3.96	5.24	3.66
	1	3.12	3.42	5.03	1.01	7.81	0.89

Figure 10 shows the power spectra measured at the error microphone positions when they are placed at a distance of 0.2 m from the open window. When 8 error microphones are used in the mixed-error implementation, only the results of 4 error microphones (No. 1 to No. 4) are plotted. The collocated and mixed-error implementations are confirmed to converge to similar residual noise levels. Figure 11 further shows the averaged power spectra measured at the 4 error microphone positions when the error microphones are placed at different distances. When the error microphones are placed at 0.1 m from the open window, the mixed-error implementation may fail to reduce the frequency band from 1.2 kHz and above. This is because when the error microphones are sufficiently far from the secondary loudspeakers, there is less difference between the mixed and individual

secondary paths. Hence, the mixed secondary path can be approximately treated as the estimates of the individual secondary paths. Similarly, when the error microphones are near the secondary loudspeakers, higher frequency bands incur more discrepancies.

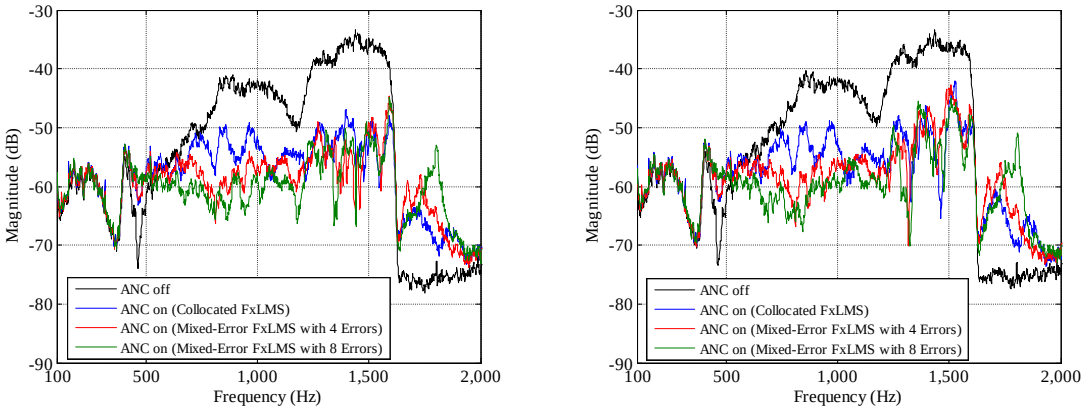

(a) Error microphone No.1

(b) Error microphone No.2

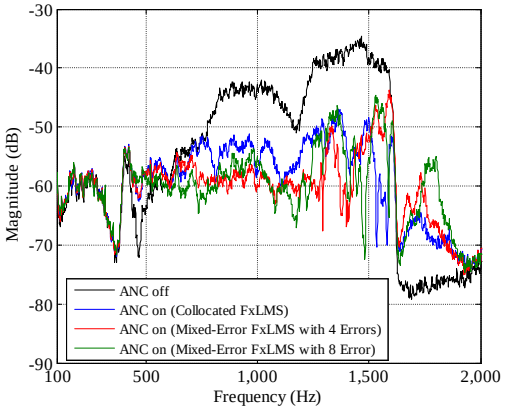

(c) Error microphone No.3

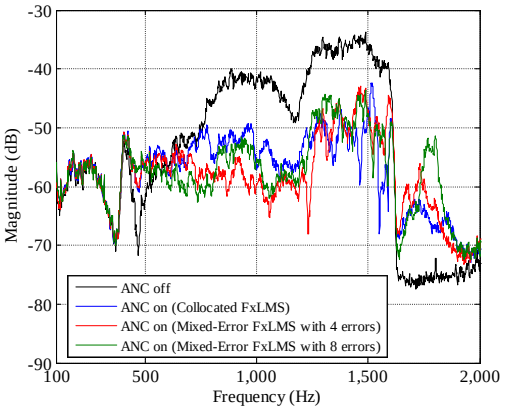

(d) Error microphone No.4

Fig. 10 Power spectra measured at the error microphone positions when the error microphones are placed at a distance of 0.2 m from the open window.

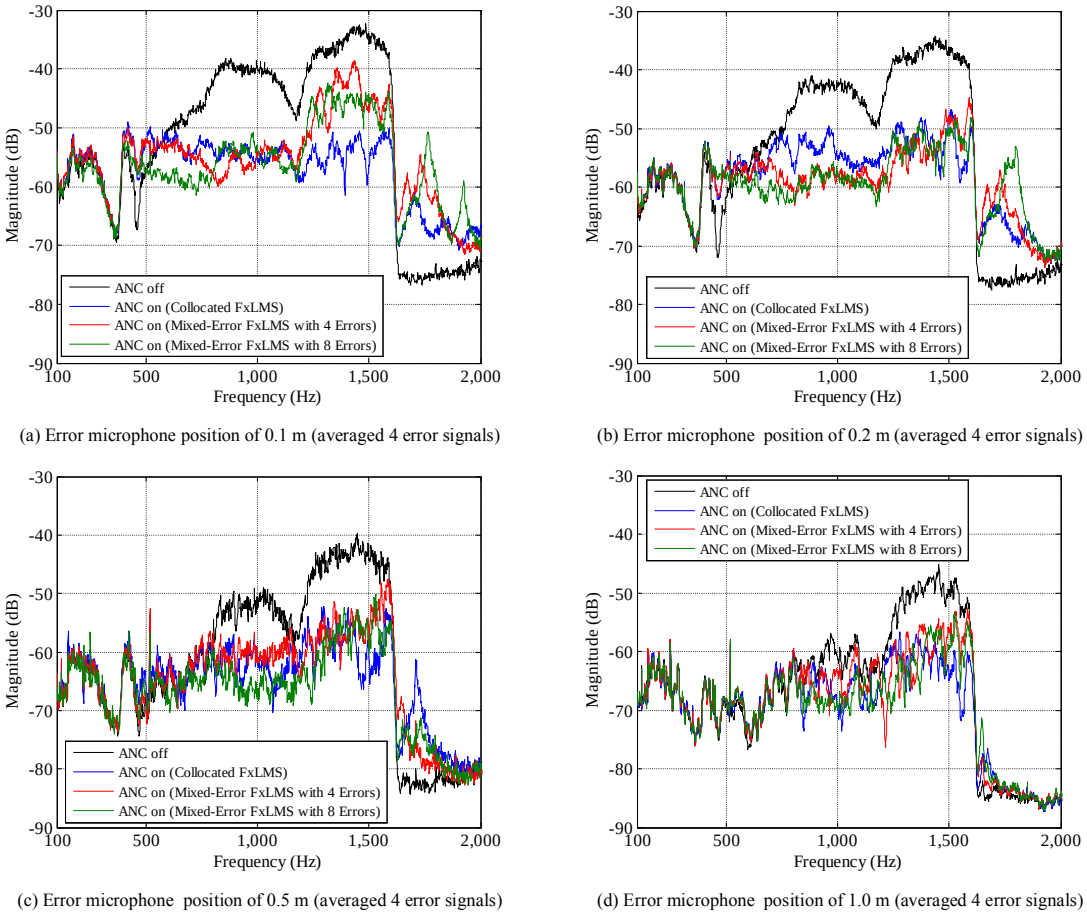

(a) Error microphone position of 0.1 m (averaged 4 error signals)

(b) Error microphone position of 0.2 m (averaged 4 error signals)

(c) Error microphone position of 0.5 m (averaged 4 error signals)

(d) Error microphone position of 1.0 m (averaged 4 error signals)

Fig. 11 Averaged power spectra at four error microphone positions when the error microphones are placed at a distance of (a) 0.1 m; (b) 0.2 m; (c) 0.5 m; (d) 1.0 m from the open window.

5. CONCLUSION

The experimental study of applying the mixed-error approach in an MCANC system for open windows has been presented with a comparison of computational complexity among the complete, collocated and mixed-error implementations. The mixed-error approach possesses the merit of the lowest computational complexity. However, the optimum control filters of the mixed-error implementation of the FxLMS algorithm have been theoretically shown to be different from those of the complete and collocated implementation of the FxLMS algorithm. Different control filters have been validated in the simulation and experiment and led to similar global noise reduction performance in the MCANC system

for open windows. In the experimental setup of a 0.2 m by 0.2 m open window, using 8 error microphones at a distance of 0.2 m can eventually lead to global noise reductions of about 10 dB by the mixed-error implementation. The collocated implementation provides similar global noise reductions at 4 to 8 times the computational cost of the mixed-error implementation, given that there are 4 secondary loudspeakers and 4 to 8 error microphones.

ACKNOWLEDGMENT

This material is based on research work supported by the Singapore Ministry of National Development and National Research Foundation under L2 NIC Award No.: L2NICCFP1-2013-7.

REFERENCE

[1] S. M. Kuo and D. R. Morgan, "Active noise control: A tutorial review," *Proc. IEEE*, vol. 87, no. 6, pp. 943-973, 1999.

[2] C. H. Hansen, "Applications of active noise control," in *Understanding active noise cancellation*. Spon Press: London, 2001, ch. 6, pp. 111-132.

[3] S. J. Elliott, "Controlling propeller and rotor noise in aircraft," in *Signal processing for active control*. Academic Press: London, 2000, ch.4, sec.8, pp. 226-232.

[4] L. J. Eriksson, "Development of the filtered-U algorithm for active noise control," *J. Acoust. Soc. Am.*, vol. 89, no. 1, pp. 257-265, 1991.

[5] J. Pan, R. Paurobally, and X. Qiu, "Active noise control in workplaces," *Acoust. Aust.*, vol. 44, no. 1, pp. 45-50, 2015.

[6] Y. Kajikawa, W. S. Gan, and S. M. Kuo, "Recent advances on active noise control: Open issues and innovative applications," *APSIPA Trans. Signal Inf. Process.*, vol. 1, no. e3, pp. 1-21, 2012.

[7] K. Tanaka, C. Shi, and Y. Kajikawa, "Binaural active noise control using parametric array loudspeakers," *Applied Acoust.*, vol. 116, pp. 170-176, 2017.

[8] J. B. Dupont and M. A. Calland, "Active absorption to reduce the noise transmitted out of an enclosure," *Applied Acoust.* vol. 70, pp. 142-152, 2009.

[9] S. Wang, J. Tao, and X. Qiu, "Performance of a planar virtual sound barrier at the baffled opening of a rectangular cavity," *J. Acoust. Soc. Am.*, vol. 138, no. 5, pp. 2836-2847, 2015.

[10] J. Tao, S. Wang, X. Qiu, and J. Pan, "Performance of an independent planar virtual sound barrier at the opening of a rectangular enclosure," *Applied Acoust.* vol. 105, pp. 215-223, 2016.

[11] F. Borchi, M. Carfagni, L. Martelli, A. Turchi, and F. Argenti, "Design and experimental tests of active control barriers for low-frequency stationary noise reduction in urban outdoor environment," *Applied Acoust.* vol. 114, pp. 125-135, 2016.

[12] C. Carme, O. Schevin, C. Romerowski, and J. Clavard, "Active noise control applied to open windows," *Proc. INTERNOISE 2016*, Hamburg, Germany, 2016, pp. 3058-3064.

[13] J. Hanselka, S. Jukkert, and D. Sachau, "Experimental study on the influence of the sensor and actuator arrangement on the performance of an active noise blocker for a tilted window," *Proc. INTERNOISE 2016*, Hamburg, Germany, 2016, pp. 3046-3057.

[14] T. Murao and M. Nishimura, "Basic study on active acoustic shielding," *J. Environment Eng.*, vol. 7, no. 1, pp.76-91, 2012.

[15] T. Murao, M. Nishimura, K. Sakurama, S. Nishida, "Basic study on active acoustic shielding: Improving the method to enlarge the AAS window," *Mechanical Eng. J.*, vol. 3, no. 1, pp. 1-12, 2016.

[16] T. Murao, M. Nishimura, J. He, B. Lam, R. Ranjan, C. Shi, and W. S. Gan, “Feasibility study on decentralized control system for active acoustic shielding,” *Proc. INTERNOISE 2016*, Hamburg, Germany, 2016, pp. 462-471.
[17] C. Shi, T. Murao, D. Shi, B. Lam, and W. S. Gan, “Open loop active control of noise through open windows,” *Proc. Meet. Acoust.*, Honolulu, Hawaii, 2016.
[18] S. Ise, “The boundary surface control principle and its applications,” *IEICE Trans. Fundamentals*, vol. E88-A, no. 7, pp. 1656-1664, 2005.
[19] P. A. Nelson and S. J. Elliott, “Active noise control: A tutorial review,” *IEICE Trans. Fundamentals*, vol. E75-A, no. 11, pp. 1541-1554, 1992.
[20] C. H. Hansen, “Number of error signals,” in *Understanding active noise cancellation*. Spon Press: London, 2001, ch. 3, sec. 5, pp. 66-67.
[21] S. M. Kuo, X. Kong, and W. S. Gan, “Applications of adaptive feedback active noise control system,” *IEEE Trans. Control Syst. Technol.*, vol. 11, no. 2, pp. 216-220, 2003.
[22] A. Siswanto, C. Y. Chang, and S. M. Kuo, “Active noise control for headrests,” *Proc. 2015 APSIPA Annu. Summit Conf.*, Hong Kong, 2015.
[23] J. Cheer and S.J. Elliott, “Spatial and temporal filtering for feedback control of road noise in a car,” in *Proc. 19th Int. Congr. Sound Vib.*, Vilnius, Lithuania, 2012